

Corrosion Failure Analysis of CuNi 90/10 on Seawater Fire Protection System

Rini Riastuti¹, Alfian², Rizky Rama Putra Manurung³, Wahyu Budiarto⁴, Agus S Kaban⁵

^{1,3,5}Department of Metallurgical and Materials Engineering, Universitas Indonesia, Depok 16424, Indonesia

²Corrosion & Material Engineer, PT. Korosi Specindo

⁴Department of Mechanical Engineering, Politeknik Masamy Internasional, Banyuwangi 68418, Indonesia

*Corresponding author, e-mail: riastuti@metal.ui.ac.id¹

Abstract—The failure analysis of a seawater fire protection system of oil and gas processing facility was observed in this paper. The fire protection pipe line & hull seawater filter were made of CuNi 90/10. Severe deep pits and fracture were observed at bottom of jockey pump spool pipe and hull seawater filter. Visual observation, scanning electron microscope, energy dispersive spectroscopy, x-ray diffractometry were employed in the present failure analysis. The oxygen exposure on CuNi 90/10 of Seawater Fire Protection system had a significant impact on failure and was exacerbated by the presence of chloride exposure.

Keywords: CuNi 90/10, Seawater, Oxygen Corrosion, Chloride

INTRODUCTION

Fire protection system is a very strategic part of a plant. In an emergency, an active and running fire suppression system is essential. Fire water pipes, as an important part of a firefighting system, are of great importance in terms of the integrity and safe operation of the installation. Therefore, fire water pipes are always under strict supervision and maintenance. In the event of a leak, the relevant line section will be shut down and immediate action taken to repair the leak and get the line operational again. The number of shutdowns is then considered a critical reliability and operational issue. What distinguish fire water pipes from other water pipes is that the water in the fire water pipes is often still and stagnant for a long time, because the fire water system is expected to be on standby and ready to deal with emergency situations. Failures in firewater systems have become a major concern in many factories. Chemical composition of water, pipe materials and microbiological factors are important issues in having a reliable and functional fire water pipe. Seawater not only contains many elements on earth such as oxygen, salinity, sulphide, but also organic molecules and marine living beings. CuNi 90/10 is the most common type of material used in seawater systems due to its

resistance to pitting corrosion and anti-fouling properties. The corrosion resistance of CuNi 90/10 material is technically caused by two factors, the first is the difficulty of ionizing due to the positive equilibrium potential and thermodynamic stability of Cu atoms. the second is the presence of Ni atoms which can increase the resistance of Cu₂O films (Bahrami et al., 2021; Jin et al., 2019; Zhu & Lei, 2001).

METHODS

Visual examination

The fire protection system permanently pressurized by the Duty/Stand-by Electrical Jockey Pumps (one continuously operating and one in stand-by). They are rated to deliver 40 m/h at 13 barg. The stand-by jockey pump will start automatically when duty jockey pump fails or pressure at the PIT-507 will reach 12.3 barg (10.64 barg at ring main level). The seawater is drawn from Buffer tanks filled by the Seawater Lift Pumps and is boosted in pressure by 2 x 100% Duty/Stand-by Jockey pumps to suit the firewater system requirement of one hydrant operating in any location with full opening nozzle without starting main Firewater Pumps. Jockey pumps pressurize the main ring with sodium hypochlorite treated seawater to prevent marine

growth developing within the distribution network. Figure 1 shows the simple diagram of the fire protection system. The treated seawater analysis of the fire protection system was listed in the Table 1. Figure 2 shows fractures and pits that occur in hull seawater filter and the jockey pump spool pipe of seawater fire protection system. This case keeps happening on this system. Surface treatment has been carried out using Belzona on the inside to reduce the corrosion rate that continues to occur. The chemical composition of Belzona was listed in the Table 2.

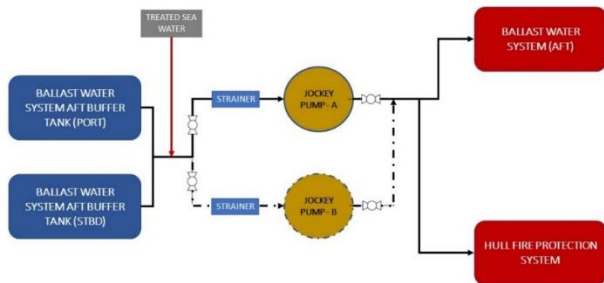


Figure 1. Simple diagram of the fire protection system

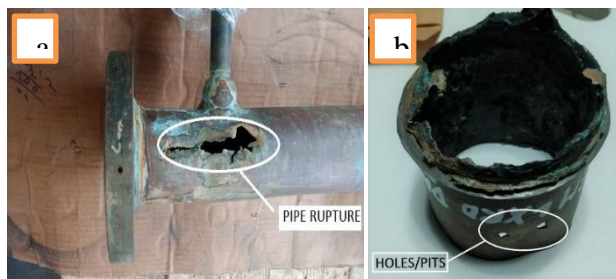


Figure 2. Failure at (a) Hull Sea Water Filter, (b) Jockey Pump spool

Table 1. Seawater Analysis

No	Parameter	Test Method	Value
1	pH	-	6.74
2	Conductivity	µS/cm	5012
3	TDS	ppm	2913
4	Sulfide	µg/L	9
5	Sulphate Reducing Bacteria (SRB)	Col/ml	Low
6	Fluid Velocity	m/s	Jockey Pump's Suction = 1.36 Jockey Pump's Discharge = 2.01

Table 2. Chemical composition of Belzona

No	Compound	% Weight
1	Bisphenol A-(Epichlorhydrin)	10 - 30
2	Amorphous Silica	1 - 5
3	Epoxy Phenol Novolac Resin	10 - 30

RESULTS

SEM & EDS Analysis

Characterization specimens are taken and prepared from the surface of the corroded material with dimension 20 x 20 x 5 mm.

Cutting of material using a grinder and no etching or other surface preparation applied prior to the examination process. Scanning Electron Microscope (SEM) conducted using Quanta 650 SEM and Energy Dispersive Spectroscopy (EDS) using Xplore 15 oxford instrument. SEM & EDS result shown in Figures 3 and 4.

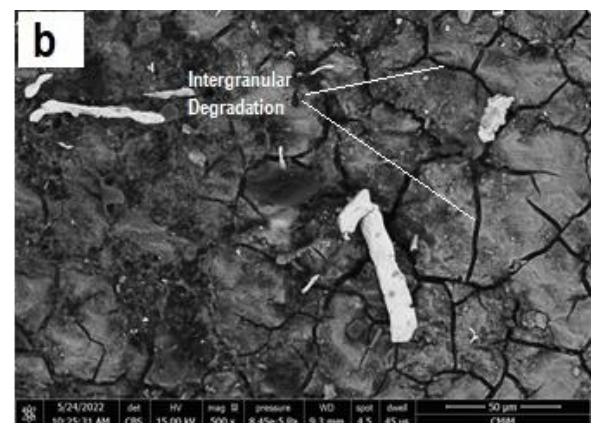
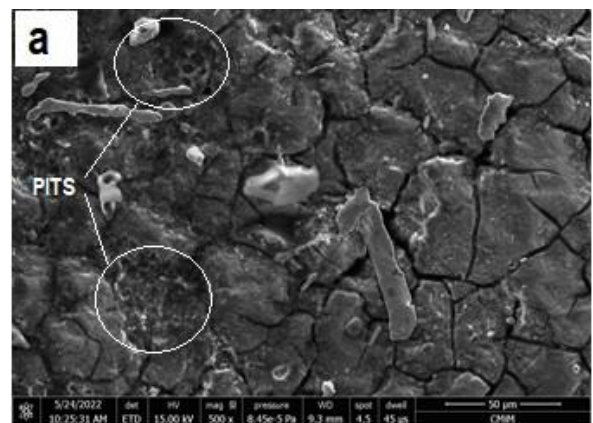
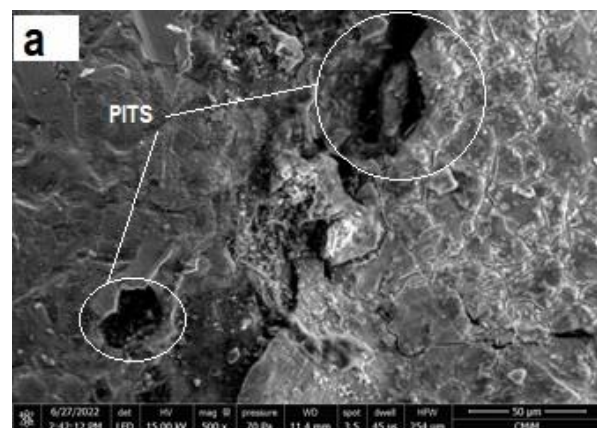


Figure 3. (a) Secondary Electrons (SE) with mag. 500X, (b) Backscattered-Electron (BSE) with mag. 500X of Jockey pump specimen



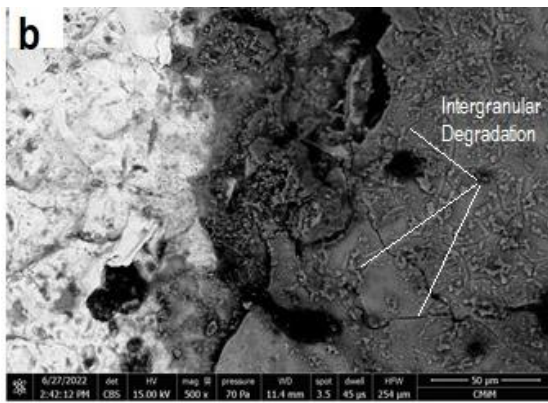


Figure 4. (a) Secondary Electrons (SE) with mag. 500X, (b) Backscattered-Electron (BSE) with mag. 500X of Hull Sea Water Filter Specimen

XRD & OES analysis

X-Ray diffractometry (XRD) technique for crystal phase analysis using X-Ray diffractometer PANalytical Aeris Suite vs. 1.4b been applied on plate specimen with a length of 20 mm, a width of 20 mm and a thickness 5 mm from the surface of the corroded material. Optical Emission Spectrometer (OES) conducted using Foundry Master Pro - Oxford Instrument. OES been conducted on bare CuNi 90/10 material with a length of 20 mm, a width of 20 mm and a thickness 5 mm. XRD result of the specimens for phase fraction shown in Tables 3 and 4. Chemical composition result of bare CuNi 90/10 material shown in Table 5

Table 3. Phase fraction of Jockey pump specimen

Atom	Density	Weight (%)
Nickel	84.760	39.09 ± 6.9179
Copper	90.716	46.05 ± 5.1600
Iron	82.623	7.38 ± 0.6595
Wustite	58.689	2.96 ± 0.4242
Tenorite	68.972	4.52 ± 0.3959

Table 4. Phase fraction of Hull Sea Water filter specimen

Atom	Density	Weight (%)
Nickel	81.708	1.66 ± 0.3779
Copper	89.774	79.66 ± 0.7947
Lepidocrocite	40.190	1.44 ± 0.7489
Goethite	42.243	1.66 ± 0.7137
Paratacamite	36.963	15.64 ± 2.5053

Table 5. Chemical composition of CuNi 90/10

Specimen	Cu	Ni	Fe	Mn	Zn	Pb	Oth
Jockey Pump	84,3	12,5	2,14	0,811	0,0095	0,0115	0,374
Hull Sea Water Filter	84,8	12,5	1,76	0,738	0,0422	0,0086	0,088
ASTM	R	9-11	1-1,8	Max 1	Max 1	Max 0,05	

DISCUSSION

Material Composition

Based on Table 5, there is an excess of Ni and Fe content. Referring to ASTM standard, percent of Ni in CuNi 90/10 material is in the range of 9 – 11 %wt. while the percent of Ni read in the OES test results is 12.5 %wt. The Fe composition range based on the standard is between 1 - 1.8 %wt, while the jockey pump specimen is 2.14 %wt. The excess composition of Ni and Fe directly allows for a deficiency in the composition of Cu in the CuNi 90/10 material. The seawater corrosion resistance offered by copper-nickel alloys results from the formation of a thin, adherent, protective surface layer that forms naturally and rapidly when exposed to clean seawater. The film is complex and consists mostly of copper oxide, often containing nickel and iron oxides, copper hydroxide and copper oxides (Karayan et al., 2011). The purpose of using Fe in CuNi 90/10 material is to improve both mechanical and corrosion properties of the alloy. The amount of iron used in this alloy is limited to a range between 1 and 1.8 %wt. because of the limited solubility of iron in the single phase as can be obtained from the Cu-Ni-Fe phase diagram (Taher, 2016). The addition of iron, in excess of 2 %wt. leads to severe segregation, which is detrimental to corrosion resistance of the material. With the lack of Cu composition, the film formation is slow/slightly formed thereby reducing the corrosion resistance of the material in the seawater environment (Elragei et al., 2010; Ezuber et al., 2016).

Topography & Morphology Observation

The topographic and morphological imaging with SEM as shown in Figures 3 and 4. There is a degradation, especially at the grain boundaries (intergranular). The degradation that occurs looks like cracks that spread along the grain boundaries. There are also pits which were marked with black imaging which showed deep topography. Intergranular corrosion is a common characteristic for copper alloy material in seawater environment (Zhu & Lei, 2001). Corrosion occurs starting at the grain boundaries, then continues to spread to the

surface to form a layer of copper oxide. At the beginnings, the layer formation was uneven and the adsorption of Cl^- ions was also inconsistent. Nickel corrosion occurs on the pipe surface causing decreased surface protection in some areas. The Cu_2O film is divided into an inner layer and an outer layer, where the outer layer is produced by the deposition of dissolved Cu^{2+} while the inner layer is produced by a more compact and protective Cu_2O film. The grain boundaries or other defects in the Cu matrix are below the corrosion product film. The growth rate of the corrosion product film in this area is slower than in the intergranular due to differences in structure and composition. When the corrosion time is extended, oxidation products in the outer layer are formed on the surface and the content is gradually increased. However, the strength of the corrosion product film is lower than its internal stress, so the product is porous and easy to fall off which causes cracks in the film (Jin et al., 2019). Cracks that occur at grain boundaries will damage the passive layer and cause pitting initiation (Kong et al., 2018).

Dissolved Oxygen & Chloride

Referring to EDS results shown in Figures 5 and 6 seen that several compounds which trigger damage due to corrosion, both general and local, including oxygen and chloride. The specimen surface has significantly higher degree of both oxygen & chloride enrichment. CuNi has excellent corrosion resistance in seawater environments. Besides Cu has a high potential value (so that the oxidation process is difficult). The presence of Nickel can also increase the resistance of the Cu_2O passive layer formed on CuNi metal. The corrosion process on CuNi can occur due to the presence of Chloride ions and large dissolved oxygen. Although the reaction of Cu and Oxygen can form a passive layer, the presence of a lot of oxygen can trigger oxidation because the electrode potential of Cu is more negative when compared to oxygen. The presence of Cl ions can exacerbate the situation by damaging the Cu_2O passive layer. Corrosion by dissolved oxygen occurs early on CuNi metal in the seawater environment by forming CuO, Cu_2O . Furthermore, the corrosion process continues with the formation of pitting since the dissolved oxygen in the system accelerated the pitting corrosion of the pipe. Corrosion products on CuNi generally have many layers. The inner layer is evenly brick red and sometimes turns black due to the superposition of the red and black layers. The passive layer on CuNi with the naked eye looks brownish yellow. In the presence of Cl ions and

dissolved oxygen, the red-black passive layer breaks down and causes the pit to deepen. Corrosion products and a greenish layer often form when corrosion is serious and ongoing (Jin et al., 2019; Subai et al., 2014) as seen in Figure 2. Copper reacts with oxygen to form a passive layer of CuO or Cu_2O with nickel as a stabilizer of the layer. It is common, the corrosion layer of Cu/Ni 90-10 is characterized by the significantly higher degree of iron enrichment resulting in the increased depletion of copper (Drach et al., 2013). This is in line with the results of the EDS analysis where there is a reduction in the composition of copper & nickel but on the contrary, there is an increase in the composition of Fe.

Table 3 and 4, It can be seen that in addition to the main elements of copper alloy material such as Cu, Ni, Fe, other compounds with small mass fractions were found to be considered. These compounds including 2.96 %wt. Wustite (FeO) & 4.52 %wt. Tenorite (CuO) found in jockey pump, 1.44 %wt. Lepidocrocite ($\gamma\text{-Fe}^{3+}\text{O}(\text{OH})$), 1.66 %wt. Goethite ($\alpha\text{-Fe}^{3+}\text{O}(\text{OH})$) and 15.64 %wt. Paratacamite ($\text{Cu}_3(\text{Cu,Zn})(\text{OH})_6\text{Cl}_2$) found in Sea Water filter specimens.

Wustite (FeO) is formed at high temperatures during the fabrication of steel, formed as a thin but very adherent layer closest to the steel surface and not a marker of oxygen ingress (Publication, 2017). Goethite is a corrosion product of the iron oxide hydroxides that forms in environments with a lot of oxygen content. Tenorite is a corrosion product of copper alloy which is commonly formed in marine environments along with cuprite (Publication, 2017; Zhong et al., 2018). In some studies, tenorite is generally formed in environments with high oxygen content and at high temperatures (annealing processes) (Jin et al., 2019; Pierson et al., 2003). Similar to Goethite, Lepidocrocite is a compound of iron oxide hydroxides which is generally formed in environments with high oxygen levels such as the atmosphere. Generally, the formation of Lepidocrocite will occur earlier, then Lepidocrocite will transform to form Goethite with increasing exposure time (Thandar et al., 2022). Another study states that Lepidocrocite in Cooper alloy is formed due to the presence of Fe^{2+} dissolved in seawater as a pollutant (Schleich, 2004). Paratacamite is a corrosion product/passive layer which is generally formed due to atmospheric corrosion in the marine environment (Petitmangin et al., 2021). Atmospheric corrosion is a type of corrosion that occurs due to high oxygen content. Paratacamite is

a stable form of copper salts at pH and temperature in deep seawater. Paratacamite is the typical precipitate from strongly acidic solutions. The Cl^- activity in seawater is high enough to inhibit the recrystallization of atacamite to paratacamite (Dekov et al., 2011).

Micro-organism, Solid Particles & Fluid Velocity

Sulphur compounds that are read on the EDS results are relatively very small around 0.4% for Jockey pump and 0.6% for Hull Sea water filter specimen, see Figures 5 and 6. In addition, since copper alloys are good biofouling inhibitors (Drach et al., 2013), this is also supported by the quality of seawater that been treated to reduce microbes in the fire protection system, which is indicated by the low results of SRB check in water analysis reports, see Table 1. SRB may be formed due to under deposit corrosion carried by seawater at small or stagnant fluid velocity (below 1 m/s). On the other hand, in case of copper alloys, it has been generally recognized that increasing flow velocities have no significant effect on the corrosion rate until a critical velocity so called breakaway velocity is reached. The maximum fluid velocity in CuNi 90/10 systems are known to be limited to 3.5 m/s (Schleich, 2004). Based on Table 1, the seawater fluid velocity of the fire protection system is within the recommended range. where the lower limit of the fluid velocity (below 1 m/s) can allow deposits to occur and the upper limit of the fluid velocity (3.5 m/s) which can allow corrosion-erosion to occur.

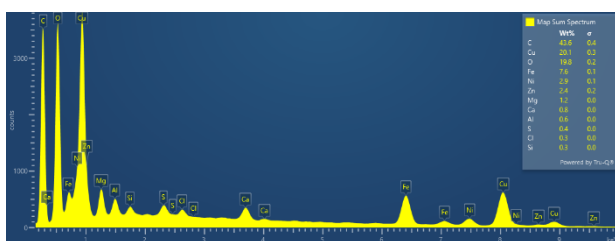


Figure 5. EDS Spectrum of jockey pump specimen

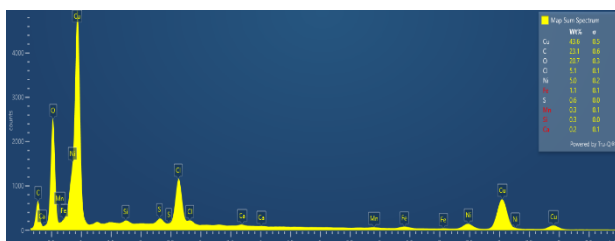


Figure 6. EDS Spectrum of hull Sea Water filter specimen

Impurities

The carbon compounds detected in the EDS test have a very large mass composition in both specimens (jockey pump and hull sea water filter). The composition of carbon compounds may be very small or even absent both in the composition of the material and in the service fluid (sea water). The large carbon compounds that can be read on the EDS is probably a compound of Belzona. As in Table 2, 2 of the 3 main compositions of Belzona (Bisphenol A-(Epichlorhydrin) & Epoxy Phenol Novolac Resin) are organic compounds (carbon bonds).

CONCLUSION

The pit and fracture occurred in the spool jockey pump fire-protection system were mostly caused by the corrosion phenomenon due to the large amount of oxygen contained in the fluid service (sea water). The presence of chloride content in seawater exacerbates the corrosion process, especially as the cause of pits. Other damage mechanisms such as micro-bacteria, solid particles, flow service, pressure & temperature do not have a large enough impact on the corrosion phenomenon of this system.

The composition of the CuNi 90/10 material that does not meet ASTM standards which can reduce corrosion resistance also exacerbates the phenomenon of failure due to corrosion. The presence of Wustite (FeO) can be concluded as an impurity/residual result of the manufacturing process for CuNi 90/10 material. The large composition of carbon compounds on the surface of the material is derived from Belzona.

REFERENCES

- Bahrami, A., Khouzani, M. K., & Harchegani, B. B. (2021). Establishing the root cause of a failure in a firewater pipeline. *Engineering Failure Analysis*, 127(April), 105474. <https://doi.org/10.1016/j.engfailanal.2021.105474>
- Dekov, V., Boycheva, T., Hålenius, U., Petersen, S., Billström, K., Stummeyer, J., Kamenov, G., & Shanks, W. (2011). Atacamite and paratacamite from the ultramafic-hosted Logatchev seafloor vent field (14°45'N, Mid-Atlantic Ridge). *Chemical Geology*, 286(3–4), 169–184. <https://doi.org/10.1016/j.chemgeo.2011.05.002>

- Drach, A., Tsukrov, I., DeCew, J., Aufrecht, J., Grohbauer, A., & Hofmann, U. (2013). Field studies of corrosion behaviour of copper alloys in natural seawater. *Corrosion Science*, 76, 453–464. <https://doi.org/10.1016/j.corsci.2013.07.019>
- Elragei, O., Elshawesh, F., & Ezuber, H. M. (2010). Corrosion failure 90/10 cupronickel tubes in a desalination plant. *Desalination and Water Treatment*, 21(1–3), 17–22. <https://doi.org/10.5004/dwt.2010.1156>
- Ezuber, H. M., Al-Shater, A., Murra, F., & Al-Shamri, N. (2016). Corrosion Behavior of Copper-Nickel Alloys in Seawater Environment. *16th Middle East Corrosion Conference & Exhibition, February*.
- Jin, T., Zhang, W., Li, N., Liu, X., Han, L., & Dai, W. (2019). Surface characterization and corrosion behavior of 90/10 copper-nickel alloy in marine environment. *Materials*, 12(11). <https://doi.org/10.3390/ma12111869>
- Karayan, A. I., Hersuni, A., Adisty, D., & Yatim, A. (2011). Failure analysis of seawater inlet pipe. *Journal of Failure Analysis and Prevention*, 11(5), 481–486. <https://doi.org/10.1007/s11668-011-9484-6>
- Kong, D., Dong, C., Zheng, Z., Mao, F., Xu, A., Ni, X., Man, C., Yao, J., Xiao, K., & Li, X. (2018). Surface monitoring for pitting evolution into uniform corrosion on Cu-Ni-Zn ternary alloy in alkaline chloride solution: ex-situ LCM and in-situ SECM. *Applied Surface Science*, 440, 245–257. <https://doi.org/10.1016/j.apsusc.2018.01.116>
- Petitmangin, A., Guillot, I., Chabas, A., Nowak, S., Saheb, M., Alfaro, S. C., Blanc, C., Fourdrin, C., & Ausset, P. (2021). The complex atmospheric corrosion of α/δ bronze bells in a marine environment. *Journal of Cultural Heritage*, 52, 153–163. <https://doi.org/10.1016/j.culher.2021.09.011>
- Pierson, J. F., Thobor-Keck, A., & Billard, A. (2003). Cuprite, paramelaconite and tenorite films deposited by reactive magnetron sputtering. *Applied Surface Science*, 210(3–4), 359–367. [https://doi.org/10.1016/S0169-4332\(03\)00108-9](https://doi.org/10.1016/S0169-4332(03)00108-9)
- Publication, N. (2017). *NACE Publication 21413 Prediction of Internal Corrosion in Oilfield Systems from System Conditions* (Vol. 5145, Issue 21413).
- Schleich, W. (2004). Typical failures of cuni 90/10 seawater tubing systems and how to avoid them. *EUROCORR 2004 - European Corrosion Conference: Long Term Prediction and Modelling of Corrosion*, 0049(0).
- Subai, S. Al, Barai, K., & Murillo, E. M. (2014). Failure analysis of firewater pipeline. *Case Studies in Engineering Failure Analysis*, 2(2), 144–149. <https://doi.org/10.1016/j.csefa.2014.07.002>
- Taher, A. M. (2016). Effect of alloying elements on the hardness property of 90% copper-10% nickel alloy. *Materials Science Forum*, 872, 13–17. <https://doi.org/10.4028/www.scientific.net/MSF.872.13>
- Thandar, W., Win, Y. Y. K., Khaing, T., Suzuki, Y., Sugiura, K., & Nishizaki, I. (2022). Investigation of Initial Atmospheric Corrosion of Carbon and Weathering Steels Exposed to Urban Atmospheres in Myanmar. *International Journal of Corrosion*, 2022. <https://doi.org/10.1155/2022/4301767>
- Zhong, X., Wang, Y., Liang, J., Chen, L., & Song, X. (2018). The coupling effect of O₂ and H₂S on the corrosion of G20 steel in a simulating environment of flue gas injection in the xinjiang oil field. *Materials*, 11(9). <https://doi.org/10.3390/ma11091635>
- Zhu, X., & Lei, T. (2001). Seawater corrosion of 70Cu-30Ni alloy of incomplete recrystallization of intermittent and full immersion. *Werkstoffe Und Korrosion*, 52(5), 368–371. [https://doi.org/10.1002/15214176\(200105\)52:5<368::aid-maco368>3.0.co;2-4](https://doi.org/10.1002/15214176(200105)52:5<368::aid-maco368>3.0.co;2-4)